

Nonlinear currents in Voronoi networks

M. Bartkowiak* and G. D. Mahan

Solid State Division, Oak Ridge National Laboratory, P. O. Box 2008, Oak Ridge, Tennessee 37831-6030 and Department of Physics and Astronomy, The University of Tennessee, Knoxville, Tennessee 37996-1200

(Received 3 October 1994; revised manuscript received 11 January 1995)

A realistic model of transport properties of zinc oxide ceramic varistors is constructed from two-dimensional Voronoi networks, with a varying degree of disorder, and studied via computer simulations. The relationship between the current-voltage (I - V) characteristic of a single grain boundary and the I - V characteristic of the network has been determined. It is found that the breakdown voltage of the network decreases rapidly when the disorder increases. The ratio of the breakdown voltage per grain boundary, calculated from the average grain size, to the actual single barrier voltage approaches the value observed experimentally in the limit of a fully random network. Moreover, the difference between these two voltages obtained from the simulation has been expressed as a function of the standard deviation of the average grain size and compared with experimental curves, showing a very good agreement. It has been found that in the breakdown region varistor networks with nonuniform grain structure conduct the current almost exclusively through very narrow channels (paths). This current localization effect decays when the applied voltage becomes very high and the network enters the upturn region.

I. INTRODUCTION

Zinc oxide varistors are multicomponent ceramic devices with highly nonlinear current-voltage (I - V) characteristics. They are produced by sintering ZnO powder together with small amounts of other oxide additives (such as Bi₂O₃ or Pr₆O₁₁, MnO₂, Co₃O₄, etc.). The resultant structure contains semiconducting n -type ZnO grains surrounded by insulating barriers at the grain boundaries. Due to the excellent nonlinear electrical properties, and very high current and energy absorption capabilities, ZnO varistors are widely used as surge arresters. A general review of the fabrication, microstructure, electrical behavior, and applications of metal-oxide varistors is given in Ref. 1.

The non-Ohmic behavior of ZnO varistors is related to specific properties of the grain boundaries in the polycrystalline sintered material. The additives form double Schottky barriers at the grain boundaries and the extreme current nonlinearity results from minority carrier creation in the barrier region.² Therefore, each grain junction is a little varistor. However, the ceramic material is a complex multijunction device composed of a large number of nonlinear elements connected in parallel and in series; very little is known about the relationship between the properties of a single junction and the global behavior of the complicated random networks of nonlinear junctions, which represent real varistor samples. A better understanding of such systems can be gained through numerical simulations; this is the object of the present paper.

In the proposed model, the polycrystalline structure of ZnO varistors is described in terms of disordered two-dimensional (2D) Voronoi networks, where Voronoi polygons represent grains of a ceramic. Nonuniformities in the grain structure are modeled by varying the degree of disorder of the Voronoi networks. We assume that each

grain boundary has a nonlinear I - V characteristic typical for varistor single grain junctions. We study transport properties of a network of such junctions via computer simulations. The model and the applied numerical procedures are described in Sec. III. As a result of the simulations, we obtain the complete I - V characteristics of the networks and a detailed insight into the current distributions in real grain-boundary barrier devices. In particular, in Sec. IV we determine the relationship between the breakdown voltage of ceramic samples, and the single-barrier voltage. Comparison of our results with the experimental data shows a very good agreement. In Sec. V, we present an analysis of the I - V characteristic of a representative disordered network and describe mechanisms of current conduction through ceramic varistors. We show that for voltages just above the breakdown of a network, the majority of the current becomes localized in very narrow paths. This phenomenon and its experimental implications are discussed in Sec. VI.

II. BACKGROUND

Typically, in the current-voltage characteristics for bulk ZnO varistors, three regions can be distinguished. At low voltages, the insulating barriers between the grains result in a very high and almost Ohmic resistivity, which is called the prebreakdown or Ohmic region. At a certain value of voltage, called the breakdown voltage, the system enters the breakdown region in which the current increases dramatically. The dependence of current upon voltage here is often described by an empirical relation

$$I = kV^\alpha, \quad (1)$$

where the parameter

$$\alpha = \frac{d(\log I)}{d(\log V)} \quad (2)$$

is a measure of the device nonlinearity. It varies with voltage and can attain values as high as 100 under special conditions.³ In these first two regions, the resistance is provided by grain boundaries. At still higher current densities, the voltage starts to increase again yielding the upturn region of the I - V characteristics. This voltage increase gradually becomes linear with current (i.e., Ohmic) and is associated with the resistivity of the ZnO grains, i.e., the upturn represents the voltage drop in the grains. Microcontact measurement upon single grain boundaries have been undertaken by many groups and have confirmed that breakdown is associated with the boundaries. Electrical characteristics of single grain junctions are similar to the ones observed for bulk ceramics. However, properties of different single barriers in the same sample may be quite different. Relatively wide variations in the single-barrier breakdown voltage and in α have been observed, as well as Ohmic junctions.⁴⁻⁸ In general, both the breakdown voltage per junction and the coefficient of nonlinearity α are found to be greater for isolated boundaries than for the ceramic as a whole. Moreover, the crossover between the Ohmic and the breakdown regions is often sharper for arbitrarily selected single junctions than for bulk materials. We will show that some of the above experimental facts can be explained as effects of the disordered, i.e., nonuniformly distributed grain structure.

The grain structure of a ceramic is an example of a space-filling cellular structure. One of the simplest ways

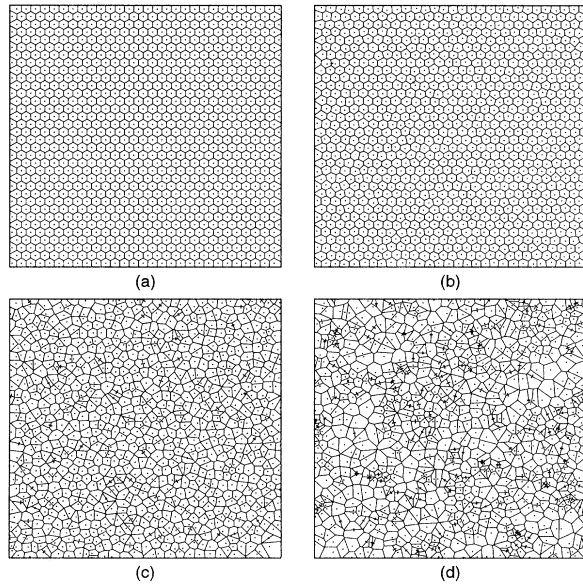


FIG. 1. Voronoi cell structure for different values of disorder parameter d (see text). (a) $d=0$ (regular hexagonal structure); (b) $d=0.18$ (deformed hexagonal structure); (c) $d=0.6$; (d) $d=8.0$, for which the structure can be regarded as generated from a fully random distribution of seed points.

to model such structures is the Voronoi construction or Voronoi tessellation.⁹ An arbitrary array of seed points is first defined, either completely random or correlated in some way. Each of these seeds is assigned a cell, in the 2D case of polygon, containing all points which are nearer to it than to any other seed. Voronoi polygons are formed by intersecting perpendicular bisectors of lines connecting neighboring seeds. This construction follows the same rules as, for example, the construction of Wigner-Seitz cells. Physically, it can be interpreted as a 2D growth process starting simultaneously at all nucleation seeds and proceeding in the plane at constant uniform rate until it is terminated whenever two approaching growth fronts reach each other. Therefore, the geometry and topology of Voronoi networks closely resemble those found in grain growth from random nucleation sites. In this way, Voronoi networks provide a natural model for the study of transport through disordered structures such as ceramic materials. The Voronoi construction also allows one to cross the whole range from regular lattice to completely random network (Fig. 1) and address the question of how disorder in the local connectivity affects the global properties across the network. Such a study for the case of linear resistor networks has been reported recently.¹⁰

III. VORONOI NETWORK MODEL OF POLYCRYSTALLINE VARISTORS

In this paper, we model electrical transport in ZnO varistors by mapping to a 2D Voronoi network. We generate the networks, consisting of 986 cells, from seed points in a square of side length $L=1$. Each cell represents a ZnO grain and each edge of the length l_{ij} shared by neighboring cells i and j corresponds to a grain boundary. Starting from a regular triangular lattice of seed points corresponding to the hexagonal cell structure shown in Fig. 1(a), disorder is introduced by displacing individual seeds within a disk of radius d around their original positions, where d is defined in units of the distance between nearest neighbors in the triangular lattice. The displacement vector has been assigned random magnitude ($\leq d$) and random direction. The total number of cells is kept constant by imposing periodic boundary conditions. For small values of d , the hexagonal cells merely become deformed [Fig. 1(b)]. When the disorder increases above $d=(\sqrt{3}-1)/4=0.183$, the lattice becomes topologically disordered,¹⁰ as the coordination number may locally deviate from its original value of six [Figs. 1(c) and 1(d)]. However, the average value of the coordination number for Voronoi lattices remains six regardless of disorder.⁶

We assume that the current passing through a grain boundary is proportional to its length l_{ij} and that all the grain-to-grain junctions have the same nonlinear I - V characteristics typical for varistor barriers. In the Ohmic and in the breakdown regions, we model these characteristics by the function

$$I(V) = V \left[\frac{(V_b)^c + V^c}{(V_b)^c} \right]^{(\alpha_{\max}-1)/c}, \quad (3)$$

where V is the voltage applied across the boundary, V_b is the breakdown voltage of the junction (barrier voltage), and α_{\max} is the maximal desired nonlinearity coefficient of single junctions. Parameter c controls the width of the crossover from the Ohmic to the breakdown region. Here we take $V_b=3$ V, $\alpha_{\max}=51$, and $c=50$. These values of the parameters give a single-junction characteristic with sharp breakdown typical for a good varistor. In the present calculation, we assume that the electrical potential is constant within a ZnO grain and that voltage drop can take place only across the grain boundaries. This is in fact equivalent to neglecting the grain resistivity. However, we have also performed simulations in which finite voltage drops in grains have been explicitly taken into account, and we have found that grain resistivity effects can be quite well modeled just by modifying the grain-to-grain junction characteristic to include an upturn region. This is the approach that we use throughout the present paper. The same basic function (3) has been used to model the junction characteristic in the upturn region. Since the crossover from the breakdown region to the upturn region is much smoother than the breakdown itself,^{3,8,11} we take $c=20$. In the ln-ln scale, we perform mirror reflections of (3) with respect to both $\ln V$ and $\ln I$ axes and shift the resultant curve in such a way that it joins curve (3) smoothly at a certain voltage $V=V_0$. This leads to the following model I - V characteristic for a single junction in the upturn region:

$$I(V) = V \left[1 + \frac{(V_0)^{50}}{(V_b)^{50}} \right]^{7/2} \left[1 + \frac{(V_0)^{70}}{(V_b)^{50} V^{20}} \right]^{-5/2}. \quad (4)$$

The value of the remaining free parameter V_0 has been set to $V_0=3.422$ V. This choice leads to a typical for varistors at room-temperatures value of order 10^{10} for the ratio between the resistance of the junction in the Ohmic region and the one in the upturn region. The grain-to-grain electrical characteristic assumed in the present study, and the nonlinearity coefficient α as a function of the voltage drop across a grain boundary, calculated from Eqs. (3) and (4), are shown in Fig. 2 as dotted curves.

An external potential difference is applied across opposite edges of the Voronoi network. Grains at the bottom and the top are given a constant potential, 0 and V , respectively. Potentials V_i of each of the other grains have to be calculated from the Kirchhoff equations

$$\sum_j l_{ij} I(V_i - V_j) = 0, \quad (5)$$

where the summation index j runs over the grains that are neighbors of grain i , and the current is calculated according to Eq. (3) when $V_i - V_j \leq V_0$, Eq. (4) when $V_i - V_j > V_0$. This leads to a large set of nonlinear equations, which we solve numerically using a simple iterative method based on a gradual adjustment of grain potentials by solving Eq. (5) locally for each V_i . The procedure converges to the global solution for the potential distribution usually after less than 2000 iterations. These results are then used to calculate the total current flowing through the network and to determine its I - V characteristic. In

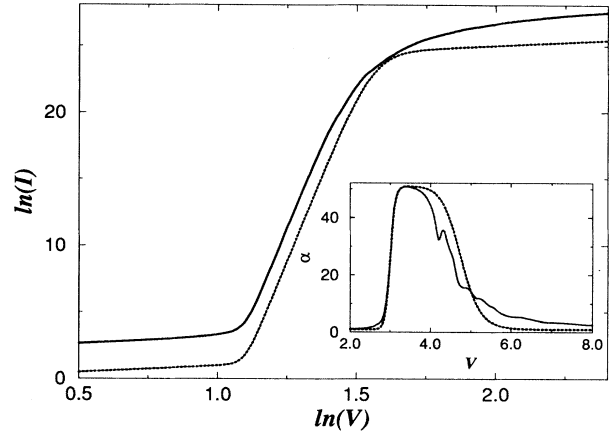


FIG. 2. ln-ln model I - V characteristic of a single grain-to-grain junction (dotted curve) and of a disordered network with $d=8.0$ (solid curve). The corresponding coefficients of nonlinearity α vs voltage are shown as an inset. The solid curves represent functions of the scaled voltage V_s [Eq. (6)]. The breakdown voltage of this network is $V_{bN}=70.95$ V.

particular, we calculate the breakdown voltage of the network. Experimentally the breakdown voltage of a varistor is defined as that for which the current density reaches 1 mA/cm^2 . Here, however, since in our simulations we deal with a 2D model, we cannot use this definition. Instead, we define the breakdown voltage of a network V_{bN} as the one for which the network nonlinearity coefficient α reaches 26—approximately half its maximal value $\alpha_{\max}=51$. Thus, V_{bN} corresponds to the position of the knee of the ln-ln I - V characteristic curve.

Moreover, we also calculate the distribution of the current on the network and, using a colored (or shaded) coding scheme, we generate its graphical image in order to visualize current paths.

IV. NETWORK BREAKDOWN VOLTAGE AND JUNCTION BARRIER VOLTAGE

For the case of the regular hexagonal grain structure [Fig. 1(a)], there are always 33 grain boundaries across the sample. Therefore, its breakdown voltage V_{bN} is exactly 99 V. No current flows across vertical junctions, and the regular network behaves just as a set of parallel conduction paths, each consisting of 33 identical varistor junctions connected in series. All the active (nonvertical) junctions enter the breakdown region and the upturn region simultaneously. Hence, apart from the simple scaling of voltage.

$$V_s = 3V/V_{bN}, \quad (6)$$

and to within a multiplicative factor appropriate for the parallel and serial connections, the I - V characteristic of the network is identical to that of a single junction. Of course, the current flows uniformly throughout the whole network and no distinct current paths are found.

However, even very little disorder in the grain structure causes dramatic change in the behavior of the network. As soon as the disorder provides alternative paths for the current, it seeks the easiest one, i.e., the path with fewest barriers between electrodes. Therefore, the electrical characteristic of the network, at least within and close to the breakdown region, is determined by the properties of such paths.

One of the experimental facts that can be attributed to the above feature of varistor networks is the discrepancy between the results of two commonly used methods of determination of the single barrier voltage. The first method consists in direct microcontact measurements and gives the real value of the barrier voltage. The second method is indirect. Knowing the breakdown voltage V_{bN} of a bulk sample of thickness D , and the average size of its grains s from optical micrographs, one should, in principle, obtain the barrier voltage as the ratio V_{bN}/n , where $n = (D/s) - 1$ is the average number of grain boundaries between the electrodes. However, the second method gives barrier voltages that are 50–70 % of the actual ones. This problem has been widely discussed in the literature.^{1,4,7,12} From the experimental point of view, it has been studied in detail by Sung, Kim, and Oh.⁷ Emage¹² has used statistical arguments to show that, due to the wide distribution of grain sizes, there is a finite density of chains of long grains through the ceramic, which act as easy paths for the current. Therefore, the effective number of grain boundaries across the sample should be smaller than the average one. Here we address the problem in terms of the proposed Voronoi network model.

In our computer simulations, the grain-size distribution and the topological disorder are controlled by the parameter d . We have computed breakdown voltages for a series of networks with different values of d . The results are presented in Fig. 3. The breakdown voltage decreases rapidly as the disorder increases, and saturates at

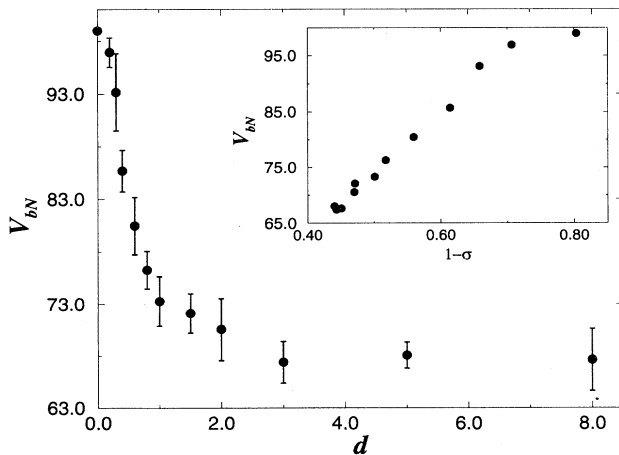


FIG. 3. Network breakdown voltage as a function of disorder parameter d . This is shown again in the inset as a function of $(1 - \sigma)$, where σ is the standard deviation of the grain-size distribution normalized by the average grain size.

about 70% of its value for the regular hexagonal lattice when the network becomes fully random. To be able to prove the discrepancy mentioned above, we have tested the indirect method of determination of the single-barrier voltage using the results of our simulation. We have calculated the average number of grain boundaries between the top and the bottom edges of each of the generated networks. The barrier voltage has then been determined by dividing the corresponding network breakdown voltage by this number. The results are presented in Fig. 4. Keeping in mind that the actual barrier voltage of each junction is exactly 3 V, we see that the indirect method gives values that are 50–70 % of the real ones, even for only slightly disordered networks. This is in very good agreement with experimental observations.^{1,7} Relatively large error bars in our data come from the statistical dispersion of the number of junctions across the networks. The error bars represent the standard deviation.

In experiments, the disorder of a ceramic is described in terms of the standard deviation of the average grain size σ . Therefore, we have transformed our results in such a way that they can be presented as a function of this measurable quantity instead of the parameter d . Grain-size distribution of the Voronoi networks has been determined by measuring lengths of segments of lines drawn across the networks, which are intercepted by grain boundaries. The same method, called the linear intercept method, is used in optical micrography.⁷ There, the data for intercept lengths are then converted to the sizes of grains in a three-dimensional (3D) ceramic by means of standard methods.¹³ However, since our networks are two-dimensional, these methods are inapplicable, and we calculate values of the average grain size and its standard deviation σ directly from the intercept

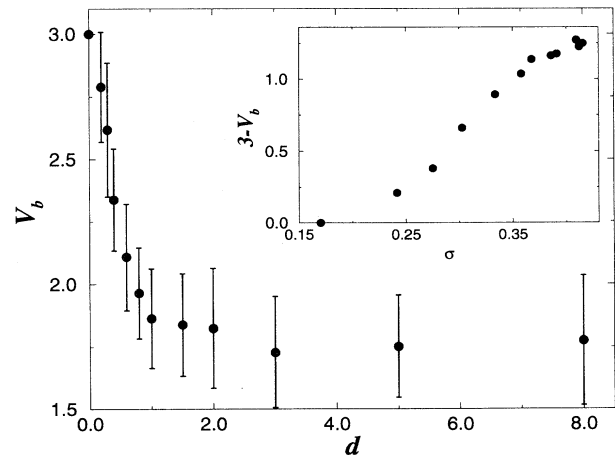


FIG. 4. Barrier voltage calculated as the ratio of the network breakdown voltage to the average number of grain boundaries across the sample as a function of d . The actual value is $V_b = 3$ V. The difference between the two values as a function of the standard deviation of the average grain size σ , is shown in the inset. Here σ is normalized by the distance between nearest neighbors in the regular triangular lattice.

lengths data. Since the average grain size of networks with the same value of d have about the same standard deviation, we can express our results in terms of σ instead of d .

As it is shown in the inset of Fig. 3, the breakdown voltage of the networks is a linear function of $(1-\sigma)$ except for the region where the networks are almost regular. This result agrees with Emtage's general conclusion derived from statistical arguments that easy current paths, which determine breakdown of the ceramic, are approximately a factor of $(1-\sigma)$ weaker than the mean path.¹² Sung, Kim, and Oh⁷ have presented experimental curves for the difference between the varistor barrier voltage measured by microcontact techniques and that calculated indirectly from the average number of grain boundaries across the sample, as a function of standard deviation of the average grain size (Fig. 8 of Ref. 7). The same curve determined from our simulations has been shown in the inset of Fig. 4. In our results, $(3-V_b)$ approaches zero for a finite value of σ at the point which corresponds to the regular hexagonal structure of the network. This is because while application of the indirect method leads to the correct result $V_b=3$ V for this case, the linear measure of sizes of the hexagons still shows a little statistical dispersion. Apart from that, the computed curve is in very good agreement with the experimental ones. This agreement indicates that properties of varistor ceramics can be quite well described by the proposed 2D model, despite the fact that the grain-size distribution for 2D Voronoi networks is not log-normal,⁹ as for the case of 3D polycrystalline ceramics.^{7,13}

V. I - V CHARACTERISTICS AND CURRENT DISTRIBUTIONS

The relationship between I - V characteristic for a single grain boundary and for the whole network is illustrated in Fig. 2. The solid curves correspond to a fully disordered network ($d=8.0$). The voltage for these curves has been scaled according to Eq. (6) for comparison with those of a single junction (dotted curves). In agreement with experimental observations, breakdown of our disordered networks appears to be somewhat less sharp than for a single junction. However, since many experimental data show much smoother crossover from the Ohmic to the breakdown region for bulk varistors, our results indicate that this rounding of the characteristics for ceramics cannot be explained exclusively by the disorder in grain structure. It is also clear that the disorder in the grain size alone is not responsible for the observed reduction in the coefficient of nonlinearity for bulk samples. The same conclusion follows from the statistical analysis of Emtage.¹² As shown in the inset of Fig. 2, maximal α for the networks is as high as for a single junction, although the interval of voltage for which it maintains the maximal value is reduced. In the present model, we have assumed that all the single grain junctions are perfect varistors. This assumption is not satisfied for the case of bismuth-type varistors, which have a multiphase structure and contain many different kind of junctions, some of them having Ohmic, instead of varistor character.^{1,5,6} There-

fore, a more realistic model of bismuth-type varistors should include some Ohmic junctions, as well as the nonlinear ones. Indeed, several numerical studies^{6,14} indicate that the nonlinearity coefficient rises much less rapidly and reaches reduced maximal values for multijunction devices in which some of the junctions are Ohmic. On the other hand, our present model should be more adequate for description of the type of varistors where only two phases, ZnO grains and thin layers of an intergranular phase, has been found.¹⁵ From our model, we anticipate that bulk polycrystalline varistors having such a two-phase microstructure should exhibit breakdown transitions almost as sharp as their single grain junctions and that the effect of reduction of α should be much smaller than that in bismuth-type varistors. Unfortunately, since no experimental microcontact measurements for these varistors have been published, to our knowledge, we cannot verify our predictions.

To gain a better insight into the process of current transport through the networks, we have calculated distribution of the current on its cell structure. The results for the structure, whose I - V characteristic was shown in Fig. 2, are presented graphically in Fig. 5. We use the following shaded coding scheme. At each cell (grain), we plot the relative value of the current passing through it, normalized by the total current flowing through the sample, and let the gray-level spectrum from white to black represent the values. For example, there is no (or almost no) current flow through cells shown as white, whereas

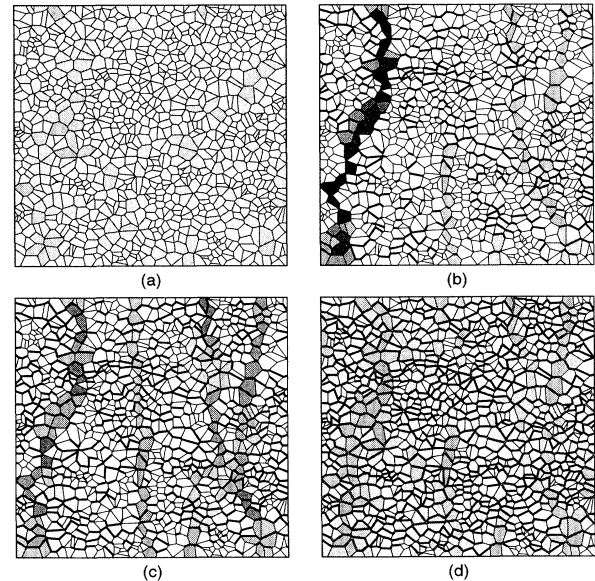


FIG. 5. Distribution of the current on a cell structure with $d=8.0$ for different applied voltages. The I - V characteristic of this structure is shown in Fig. 2. (a) $V_s=1.5$ (in the Ohmic region); (b) $V_s=3.5$ (in the breakdown region); (c) $V_s=4.3$ (entering the upturn region); (d) $V_s=6.0$ (deep in the upturn region). Explanation of the graphical coding is given in the text.

quite black cells conduct practically 100% of the total current. Boundaries between grains for which the potential difference is higher than 3 V, i.e., boundaries that are in the breakdown region, are represented in the current distribution graphs by heavy lines. When the voltage between neighboring grains exceeds the value for which the nonlinearity coefficient of the corresponding junction drops back below 26, we consider the junction as being in the upturn region. This happens for $V=4.754$ V in our model. Such boundaries are represented graphically as double lines.

For voltages in the Ohmic region [Fig. 5(a)], current flows uniformly through the whole network. The breakdown takes place gradually. At first, some of the grain junctions locally enter the breakdown. This usually happens either to the shortest grain boundaries (as the current flow is limited there and the neighboring grains develop a high potential difference), or to the boundaries that are shared by long grains oriented vertically. In this range of voltage, α starts increasing slowly (see the inset of Fig. 2). Then, for a certain voltage, a path linking opposite edges of the network appears. The path comprises only grains connected by junctions above the breakdown, and starts conducting much more current than the rest of the network. This characteristic voltage corresponds to the breakdown voltage of the network V_{bN} . A very interesting feature of this phenomenon is that although further moderate increase of voltage creates more and more paths that link the electrodes and consist of junctions above breakdown, they do not significantly contribute to the current conduction. Instead, the current becomes more and more localized in the path that appeared first. This current localization effect is shown in Fig. 5(b), where an easy path is about 1–3 grains wide and conducts over 75% of the total current. Other easy paths exist in the network, but do not conduct much of the current. The fact that the current in simple multijunction nonlinear devices can be distributed extremely nonuniformly has also been recently noticed in other numerical simulations.⁸

When the applied voltage is high enough to drive some of the junctions in the conducting easy path into the upturn region, the current is being pushed out from it, and the network itself enters the upturn region. In some cases, the current finds other secondary paths, the junctions of which are not yet in the upturn region, or not yet so deep in the upturn region. It flows through them until, with increasing voltage, the junctions of these new paths, entering deeper into the upturn region, push it out too. As a result of processes of this kind, the coefficient of nonlinearity as a function of voltage may exhibit a series of decaying oscillations and sometimes may even have local maxima, as for the case shown in Fig. 2. The current distribution portrayed in Fig. 5(c) corresponds to the voltage for which α has a local maximum, i.e., for $V_s=4.3$. Here, three of the grain boundaries in the previously highly conducting path are in the upturn region, and the current is pushed to a few secondary current paths. Consequently, the current flow is much less localized than in the breakdown region. The three grain boundaries in the upturn regions are the narrowest ones.

Therefore, it is rather difficult to see them in the low scale graph in Fig. 5(c). Finally, for a very high voltage, many junctions are deep in the upturn region, and distribution of the current become quite uniform again [Fig. 5(d)]. To our knowledge, no oscillations of α as a function of voltage in the upturn region have been observed experimentally. In fact, our simulations show that the smoother the crossover from the breakdown to the upturn region, assumed for a single-junction I - V characteristic, the less likely oscillations are to appear. It is, therefore, altogether possible that this effect is just an artifact of the model. Moreover, one can expect the oscillations to gradually smooth out when the number of grains increases because the distribution of secondary paths becomes wider and smoother.

The way in which varistor Voronoi networks enter the breakdown resembles the percolation phenomenon. The number of the grain boundaries above the breakdown gradually increases as the applied voltage grows, and finally a path along which all the junctions are at the breakdown appears between the electrodes. This might be viewed as reaching the percolation threshold. However, since the conductance of the grain boundaries remaining in the Ohmic region is not zero, whenever some of the microjunctions enter the breakdown, the voltage and current distributions adjust to the new situation. Hence, the process of transition of subsequent grain junctions into the breakdown region is not random and the positions of the grain boundaries at the breakdown are strongly correlated. Therefore, the standard random percolation theory is not applicable. On the other hand, our model can be regarded as a peculiar correlated percolation problem on a disordered two-dimensional network with highly nonlinear transport properties. Moreover, once the current path is established and the network enters the breakdown region, one can identify objects analogical to percolation clusters and percolation cluster backbones,¹⁶ and perhaps use these concepts to study scaling properties of the current distribution. These interesting problems, however, remain beyond the scope of this paper.

VI. CURRENT LOCALIZATION

Perhaps the most interesting results of our simulations is the current localization phenomenon. It is present for networks with d as low as 0.2, so we can conclude that no wide distribution of grain sizes is necessary for a network to develop an easy path. Instead of chains of long grains, we then have chains of grains connected by short boundaries. Our results indicate that the current localization effect should be very common in polycrystalline varistors. It has appeared in almost all of over 50 network models that we have studied. In the breakdown region, the current can localize in paths of many different kinds. Some of them are shown in Fig. 6. The network presented in Fig. 6(a) provides another example of a single localized path similar to that in Fig. 5(b). This is the most common situation. However, the current localization effect is extreme here. The narrow path conducts over 955% of the total current. Sometimes, a well-localized

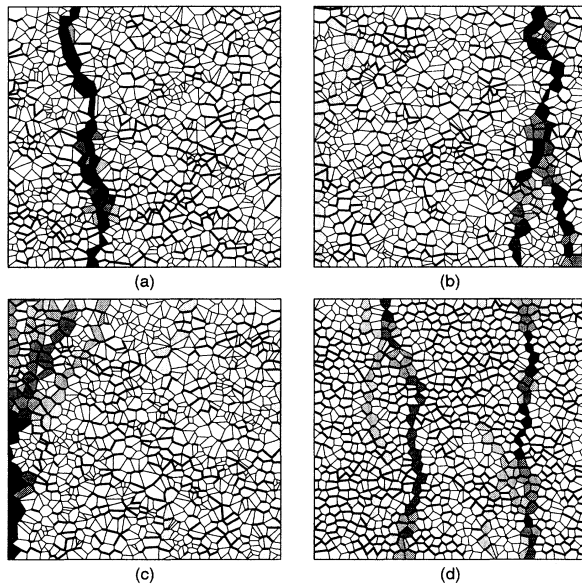


FIG. 6. Examples of distributions of the current on different cell structures in the breakdown region. (a) A single path with highly localized current for a structure with $d=5.0$; (b) A path that splits into two others ($d=3.0$); (c) A path that dissolves into the network ($d=8.0$); (d) A two-path distribution ($d=0.6$).

single path splits into two or more channels [Fig. 6(b)], or even almost disappears, dissipating the current into a large portion of the network [Fig. 6(c)]. For the case of less disorder, networks with two parallel easy paths, conducting almost 50% of the total current each, can be found. An example of such a situation is shown in Fig. 6(d). We emphasize that the two channels do not appear one after another when the network enters the breakdown region, but arise simultaneously.

Appearance of paths with highly localized current seems to be even more probable for three-dimensional polycrystalline ceramics, as with the log-normal grain-size distribution chains of long grains are more likely to exist. In fact, nonuniform current distributions on the surfaces of varistor disks have been observed and measured by applying small spot electrodes and by using infrared radiation thermocameras.^{17,18} However, those current distributions have been attributed to macroscopic nonuniformities in varistor blocks, which may appear as a result of ceramic processing. Our results, on the other hand, indicate that the observed current concentration is related to the disorder in the microscopic (grain size) scale, rather than to the macroscopic nonuniformities of varistor blocks. As our results showed, it is impossible to control disorder in the grain structure of ceramics to such an extent that the current localization effect could be avoided. Therefore, nonuniform current distribution seems to be an intrinsic feature of varistor ceramics.

A direct experimental evidence of the current localization phenomenon is provided by the electroplating (gal-

vanic) technique,¹⁹ where one side of a varistor sample is put into contact with the surface of a salt solution and acts as a cathode. A sufficient time of current flow through the galvanic circuit causes all the conductive areas of the varistor surface to become covered with metal. It turns out that metallic deposition on varistor surfaces always takes a form of very small spots,¹⁹ showing that the current flows almost exclusively through very narrow channels. On the other hand, variations of the density of the metallic spots can be used to estimate *macroscopic* uniformity of the varistor samples.

The localization of the current in narrow paths is also clearly visible from experiments in which electroluminescence images of cut surfaces of a varistor operating in its breakdown were created.²⁰ The luminescence comes from the recombination of holes produced during the electrical breakdown of the interface barriers.² Therefore, it occurs only at the grain boundaries that are above the breakdown and which conduct high current. Bright spots in the luminescence images corresponding to these grain boundaries form very distinct paths. The image presented in Ref. 20 perfectly agrees with the graphs in Fig. 6 and provides a direct experimental corroboration of our results.

Another experimental observation that can be interpreted as a consequence of the current localization is the dc bias dependence of the ac superimposed small-signal electrical response of varistors. Alim and Seitz²¹ have shown that the depression angle of the semicircular fitting of the ac small-signal electrical data represented in the impedance plane gradually decreases as increasing dc bias in the breakdown region. It finally vanishes when the dc voltage reaches approximately the value for which α is maximum. The depression angle is a representative of the degree of uniformity or nonuniformity in the lumped relaxation process between the electrodes. Therefore, one can expect it to decrease significantly when the current becomes localized in narrow conducting paths. Indeed, the observed region of the dc voltage for which the depression angle decreases and vanishes corresponds in our simulations to the one where the current localization effect takes place and intensifies.

The current localization phenomenon is of crucial importance for the energy handling capability of ZnO varistors. One of the most common destruction modes of varistor blocks is a puncture mode, which produces a very small through hole, obviously caused by melting of the region of the ceramic body where current is concentrated.¹⁷ The puncture destruction mode so closely resembles our graphs showing localized current paths, e.g., Fig. 6(a), that it can be regarded as an additional confirmation of the validity of the presented results.

ACKNOWLEDGMENTS

The authors are indebted to Dr. F. A. Modine (ORNL) and to Dr. M. A. Alim (The Ohio Brass Company) for stimulating suggestions and discussions. This research was sponsored by the Division of Material Sciences, U. S. Department of Energy under Contract No. DE-AC05-84OR21400 with Martin Marietta Energy Systems, Inc. and by Oak Ridge Institute for Science and Education.

- *Permanent address: A. Mickiewicz University, Institute of Physics, PL-60769 Poznań, Poland.
- ¹L. M. Levinson and H. R. Philipp, *Am. Ceram. Soc. Bull.* **65**, 639 (1986); T. K. Gupta, *J. Am. Ceram. Soc.* **73**, 1817 (1990).
- ²G. D. Mahan, L. M. Levinson, and H. R. Philipp, *J. Appl. Phys.* **50**, 2799 (1979); G. E. Pike, in *Grain Boundaries in Semiconductors*, edited by H. J. Jeremy, G. E. Pike, and C. H. Seager, MRS Symposia Proceedings No. 5 (Materials Research Society, Pittsburgh, 1982), p. 369; G. E. Pike, S. R. Kurtz, P. L. Gourley, H. R. Philipp, and L. M. Levinson, *J. Appl. Phys.* **57**, 5521 (1985); A. Miralles, A. Cornet, and J. R. Morante, *Semicond. Sci. Technol.* **1**, 230 (1986); G. Blatter and F. Greuter, *Phys. Rev. B* **33**, 3952 (1986); **34**, 8555 (1986).
- ³H. R. Philipp and L. M. Levinson, *J. Appl. Phys.* **48**, 1621 (1977).
- ⁴J. T. C. van Kemenade and R. K. Eijnhoven, *J. Appl. Phys.* **50**, 938 (1979).
- ⁵E. Olsson and G. L. Dunlop, *J. Appl. Phys.* **66**, 3666 (1989).
- ⁶M. Tao, B. Ai, O. Dorlanne, and A. Loubiere, *J. Appl. Phys.* **61**, 1562 (1987).
- ⁷G. Y. Sung, C. H. Kim, and M. H. Oh, *Adv. Ceram. Mater.* **2**, 841 (1987).
- ⁸H.-T. Sun, L.-Y. Zhang, and X. Yao, *J. Am. Ceram. Soc.* **76**, 1150 (1993).
- ⁹D. Weaire and N. Rivier, *Contemp. Phys.* **25**, 59 (1984).
- ¹⁰A. Pirolo, H. M. Jaeger, A. J. Dammers, and S. Radelaar, *Phys. Rev. B* **46**, 14 889 (1992).
- ¹¹P. R. Emtage, *J. Appl. Phys.* **48**, 4372 (1977).
- ¹²P. R. Emtage, *J. Appl. Phys.* **50**, 6833 (1979).
- ¹³M. I. Mendelson, *J. Am. Ceram. Soc.* **52**, 433 (1969).
- ¹⁴Z.-C. Cao and R.-S. Song, *J. Eur. Ceram. Soc.* **6**, 85 (1990).
- ¹⁵K. Mukae, *Am. Ceram. Soc. Bull.* **66**, 1329 (1987).
- ¹⁶L. de Arcangelis, S. Redner, and A. Coniglio, *Phys. Rev. B* **34**, 4656 (1986); J. Schmittbuhl, G. Olivier, and S. Roux, *J. Phys. A* **25**, 2119 (1992), and references therein.
- ¹⁷K. Eda, *J. Appl. Phys.* **56**, 2948 (1984).
- ¹⁸A. Mizukoshi, J. Ozawa, S. Shirakawa, and K. Nakano, *IEEE Trans. Power Appar. Syst.* **102**, 1384 (1983).
- ¹⁹G. Hohenberger, G. Tomandl, R. Ebert, and T. Taube, *J. Am. Ceram. Soc.* **74**, 2067 (1991).
- ²⁰F. Greuter, G. Blatter, M. Rossinelli, and F. Stucki, in *Ceramic Transactions, Vol. 3: Advances in Varistor Technology*, edited by L. M. Levinson (American Ceramic Society, Westerville, OH, 1989), pp. 31–53.
- ²¹M. A. Alim and M. A. Seitz, *J. Am. Ceram. Soc.* **71**, C-246 (1988).